

Phase-sensitive evidence for the sign-reversal s_{\pm} symmetry of the order parameter in an iron-pnictide superconductor using Nb/Ba_{1-x}Na_xFe₂As₂ Josephson junctions

A. A. Kalenyuk^{1,2}, A. Pagliero¹, E. A. Borodianskyi¹, A. A. Kordyuk^{2,3}, and V. M. Krasnov^{1*}

¹*Department of Physics, Stockholm University, AlbaNova University Center, SE-10691 Stockholm, Sweden*

²*Institute of Metal Physics of National Academy of Sciences of Ukraine, 03142 Kyiv, Ukraine and*

³*Kyiv Academic University, 03142 Kyiv, Ukraine*

Josephson current provides a phase sensitive tool for probing the pairing symmetry. Here we present an experimental study of high-quality Josephson junctions between a conventional s -wave superconductor Nb and a multi-band iron-pnictide Ba_{1-x}Na_xFe₂As₂. Junctions exhibit a large enough critical current density to preclude the d -wave symmetry of the order parameter in the pnictide. However, the $I_c R_n$ product is very small $\simeq 3 \mu\text{V}$, which is not consistent with the sign-preserving s_{++} symmetry either. We argue that the small $I_c R_n$ value along with its unusual temperature dependence provide evidence for the sign-reversal s_{\pm} symmetry of the order parameter in Ba_{1-x}Na_xFe₂As₂. We conclude that it is the phase sensitivity of our junctions that leads to an almost complete (bellow a sub-percent) cancellation of supercurrents from sign-reversal bands in the pnictide.

Symmetry of the order parameter provides one of the main clues about the mechanism of superconductivity. Attractive electron-phonon interaction leads to a simple s -wave symmetry in conventional low- T_c superconductors. Unconventional superconductivity in cuprates and iron-pnictides is characterized by a proximity to an anti-ferromagnetic state, suggesting importance of spin interactions. The corresponding direct electron-electron interaction is non-retarded and, therefore, repulsive. It was predicted that this could favor superconductivity with a sign-reversal symmetry [1–3]. In single band cuprates the sign-reversal can be only achieved with a d -wave symmetry [1, 4]. But in a multi-band pnictides the sign change may also take place between different bands, resulting in the s_{\pm} symmetry [2, 3, 5–7]. On the other hand, presence of the nematic order [8–14] suggests importance of charge/orbital interactions [15, 16], which could lead to a sign-preserving s_{++} symmetry [17]. Thus, establishing of the gap symmetry provides a key evidence towards the mechanisms of unconventional superconductivity.

At present determination of the gap symmetry in iron-pnictides remains ambiguous. For example, a resonant peak observed in inelastic neutron scattering [18–20] can be due to either a zero in the denominator of the dynamic spin susceptibility, caused by the sign-reversal order parameter, or to the nominator (Lindhard function) [21], if one takes into account quasiparticle damping [22]. Gap nodes, deduced from angular resolved photoemission spectroscopy [23] and heat conductance [24] may indicate either s_{\pm} or d -wave symmetry. Alternatively, the strong reduction of the gap can be related with the change of the orbital character from $d_{xz/yz}$ to d_{z^2-1} [25].

Josephson effect facilitates phase-sensitive probe of the order parameters [1, 4–7]. So far few reliable phase-sensitive experiments were reported for pnictides [26–29]. Both integer and half-integer flux-quantum transitions were observed [26] and large variations of the $I_c R_n$ product, where I_c is the critical current and R_n is the junction

resistance, were reported [27]. Interpretation of such results is ambiguous because half-flux quantum transitions may occur even in conventional s/s junctions due to influence of Abrikosov vortices [30], and for s/s_{\pm} junctions phase shifts depend on the tunneling direction and the $I_c R_n$ depends on tunneling probabilities from the two bands [5–7, 28]. Evidence for the s_{\pm} symmetry in pnictides were obtained via impurity-dependence of the London penetration depth [31] and quasiparticle interference patterns in STM [32, 33]. Yet, for understanding of the unconventional superconductivity in iron-pnictides there is a need of unambiguous phase-sensitive experiments. This in turn requires solution of a technological problem of fabrication of high-quality, homogeneous and reproducible Josephson junctions.

In this work we study small, reproducible and high-quality Josephson junctions between a conventional s -wave superconductor Nb and a c -axis oriented single crystal of Ba_{1-x}Na_xFe₂As₂ (BNFA). Junctions exhibit a clear Fraunhofer modulation of the critical current. Presence of significant Josephson current precludes the d -wave symmetry in BNFA. However, the $e I_c R_n$ product of junctions is very small $\sim \mu\text{eV}$, several hundred times smaller than the corresponding energy gaps. This is inconsistent with s_{++} symmetry and provides strong evidence for the s_{\pm} symmetry in BNFA. We conclude that there is an almost complete cancellation of opposite supercurrents from the sign-reversal bands in the pnictide [5–7, 28, 34]. This conclusion is also supported by observation of a specific temperature dependence of $I_c R_n$.

Figure 1 (a) shows a sketch of Brillouin zone of Ba_{1-x}K_xFe₂As₂ [35], which is similar to BNFA [36]. Fermi surface consists of three barrels in the center and a propeller-like sheets at the corners [37]. Contributions to superfluid density of corner sheets and central barrels are comparable [38]. Josephson current between an s -wave superconductor and c -axis oriented BNFA is sensitive to the signs of the gaps in different electronic bands of the

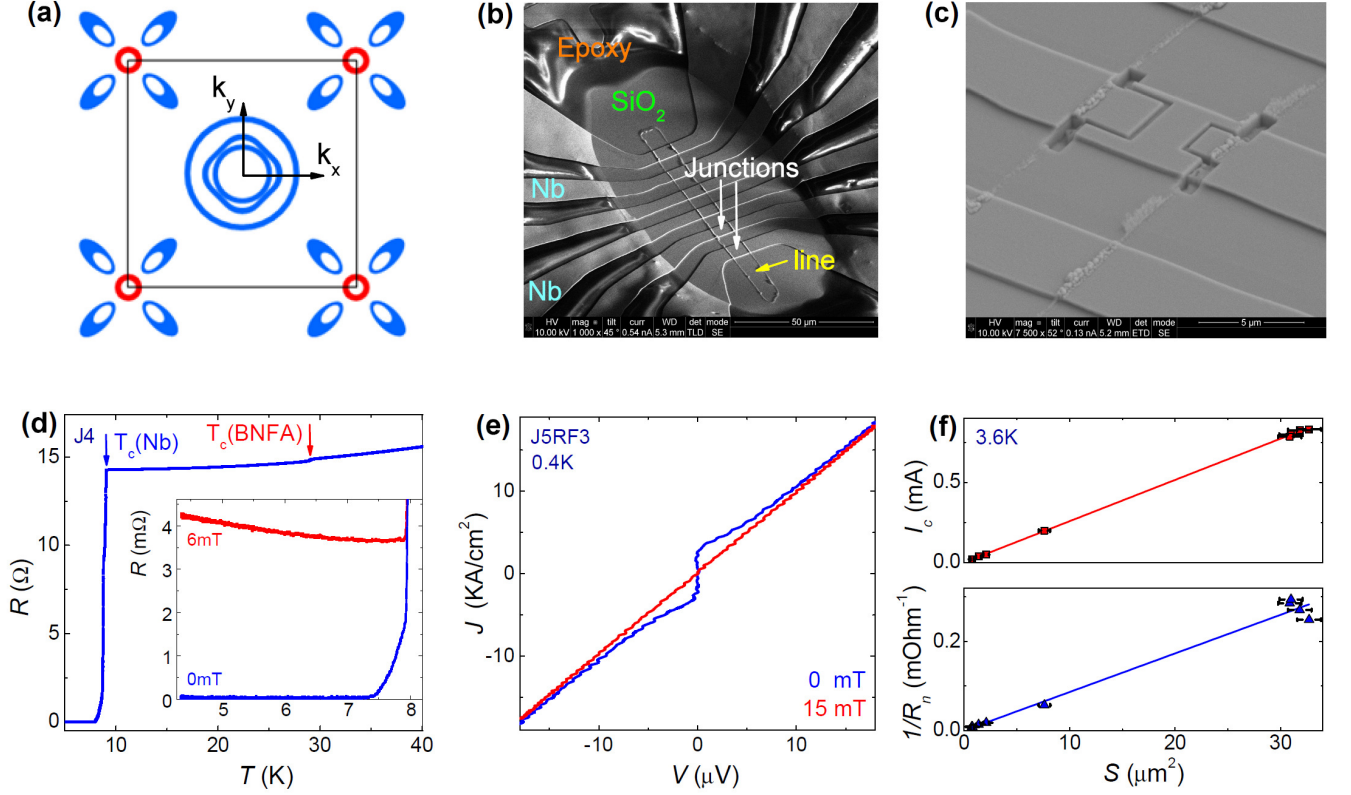


FIG. 1. (Color online). (a) A sketch of the Fermi surfaces: blue - hole type, red - electron type sheets. (b) and (c) Scanning electron microscopy images of the studied sample (b) before and (c) after FIB trimming. (c) Temperature dependence of the junction resistance. Inset shows resistance below the T_c of Nb. Blue curve at zero field. R drops to zero due to appearance of the Josephson current. Red curve is measured at field 6 mT parallel to the junction plane, at which the critical current is fully suppressed. Therefore, it represents junction resistance $R_n(T)$. (e) Current-voltage characteristics of a small FIB trimmed junction at $T \simeq 0.4$ K at zero field (blue) and at 15 mT in-plane field (red). (f) Critical current (top) and junction conductance (bottom panel) versus junction area for junctions at the same chip.

pnictide. If the gaps are of the same sign (s_{++} case) the $eI_c R_n$ should be of order of the energy gap $\Delta \sim \text{meV}$ in the s -superconductor [39]. But in the sign-reversal s_{\pm} case contributions from the bands with different signs would oppose each other [5–7, 28, 34] and we expect a smaller $eI_c R_n$. For the pure d -wave case the first harmonic Josephson current should be zero [40].

Figure 1 (b) represents a top view of the studied sample. Initially six Nb/BNFA junctions (J1-6) $\sim 6 \times 5 \mu\text{m}^2$ with two contacts each are made on top of the BNFA crystal. After initial test, the sample was transferred into a Focused Ion Beam (FIB) machine and some junctions were trimmed down to sub-micron sizes, as shown in Fig. 1 (c). This is done in order to study scaling of the junction characteristics with area. All junctions have approximately a square shape with areas from 32 to $\sim 0.1 \mu\text{m}^2$. More experimental details can be found in the Supplementary [41].

Multiterminal configuration allows simultaneous measurements of junctions and in-plane characteristics of the base crystal, as described in Refs. [41, 45]. Fig. 1 (d)

shows resistive transition of the junction J4 ($6.4 \times 5 \mu\text{m}^2$) measured in a quasi 4-probe configuration (I^+ and V^+ at two separate contacts at the same Nb electrode and I^- and V^- at two different contacts). With decreasing T we first observe a drop of resistance at $T_c(\text{BNFA}) \simeq 30$ K, when the underlying BNFA crystal becomes superconducting. The drop is small because only a small volume immediately beneath the junction is probed since the crystal contribution is measured via two different electrodes. The drop occurs at the same temperature and has the same width $\Delta T \sim 1$ K as the in-plane resistive transition of the crystal [41]. This proves that the crystal at the junction interface is not deteriorated (no proximity effect). The resistance drops to zero below $T_c(\text{Nb}) \simeq 8$ K, indicating appearance of supercurrent through the junction. Inset in Fig. 1 (d) shows $R(T)$ at $T \lesssim T_c(\text{Nb})$ at zero field and at 6 mT applied parallel to the junction interface. At this field the supercurrent is fully suppressed. Therefore, the red curve in the inset represents junction resistance $R_n(T)$. It is slightly increasing with decreasing T .

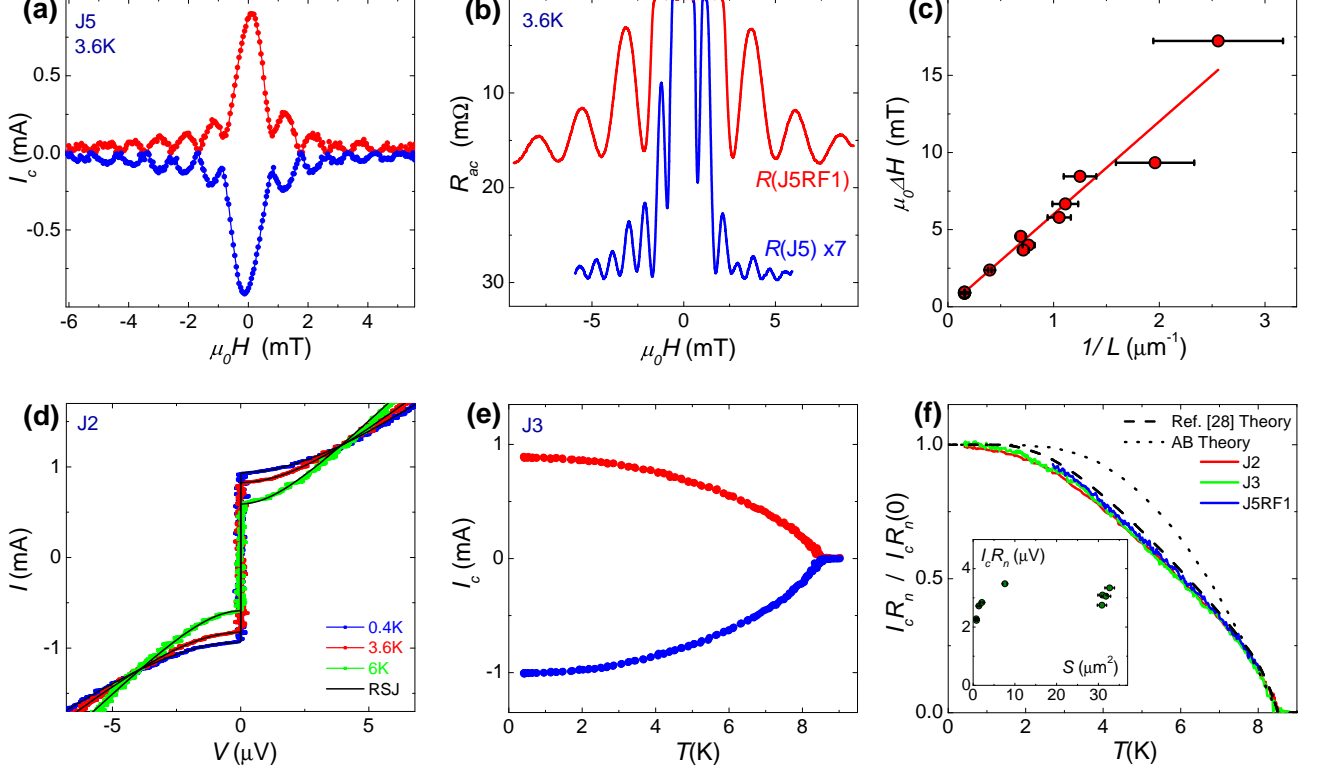


FIG. 2. (Color online). (a) Measured Fraunhofer modulation $I_c(H)$ for positive and negative currents. (b) Measured Fraunhofer modulation of ac-resistance for two junctions with significantly different sizes $L = 6.35 \mu\text{m}$ (blue) and $2.52 \mu\text{m}$ (red line). (c) Scaling of the period of Fraunhofer modulation vs. the inverse length of the junction for junctions at the same chip. (d) Current-Voltage characteristics of the J2 junction at different T . Note the slight decrease of the junction resistance with increasing T . Black line represents a fit in the resistively shunted junction model. (e) Temperature dependencies of the positive and negative critical currents at zero field. (f) Temperature dependencies of the $I_c R_n$ product, normalized by the $T = 0$ value, for three junctions. The dotted line and the dashed lines represent calculated dependencies for the sign-preserving s/s_{++} and sign-reversal s/s_{\pm} junctions, respectively (both from Ref. [28]). Inset shows $I_c R_n$ values for junctions at the same chip. It is seen that the $I_c R_n$ is very small, confirming phase-sensitive supercurrent cancellation from the sign-reversal s_{\pm} bands.

Fig. 1 (e) shows current-voltage (I - V) characteristics of a small FIB-trimmed junction ($0.95 \times 0.85 \mu\text{m}^2$). The blue curve is zero field I - V . It is non-hysteretic and have the shape typical for resistively shunted junctions (RSJ) with a clear critical current and an asymptotic Ohmic behavior at $I \gg I_c$. The red curve shows the I - V measured at in-plane field of 15 mT. Small parallel field totally suppresses I_c and the I - V becomes Ohmic. We emphasize that it is fully linear, without excess current. This again implies that there is no deteriorated interface with reduced T_c (no proximity effect), nor pinholes in the junction interface [46]. This is important because it shows that we probe bulk properties of the BNFA crystal, rather than some obscure surface layer.

Fig. 1 (f) shows critical currents and conductances $1/R_n$ versus junction area. Linear scaling demonstrates excellent reproducibility of junction characteristics.

The main fingerprint of dc-Josephson effect is Fraun-

hofer modulation of I_c versus in-plane magnetic field. Figure 2 (a) shows $I_c(H)$ dependencies for the J5 junction with the length perpendicular to field $L = 6.35 \mu\text{m}$. A clear Fraunhofer modulation is seen, indicating good uniformity of the junction [47]. The period $\mu_0 \Delta H = \Phi_0 / L \Lambda$ corresponds to a flux quantum Φ_0 in the junction. Here Λ is the magnetic thickness of the junction [41]. ΔH should be inversely proportional to the junction size L . Fig. 2 (b) shows Fraunhofer modulations (see the Supplementary [41]) for junctions with $L = 6.35 \mu\text{m}$ (blue) and $2.52 \mu\text{m}$ (red). It is seen that the period of modulation depends on L . Fig. 2 (c) shows the period versus inverse junction length (error bars reflect the uncertainty, ~ 100 nm, of determination of junction sizes). Linear dependence $\Delta H \propto 1/L$ together with scaling of I_c and $1/R_n$ with area, see Fig. 1 (f), confirms that we indeed probe junction characteristics.

Fig. 2 (d) shows temperature evolution of the I - V

curves at zero field. The shapes of I - V 's are in a perfect agreement with the RSJ model, as demonstrated by the solid black line. It is seen that both the critical current and the junction resistance R_n increase with decreasing T . The corresponding variation of $R_n(T)$ can be seen from the $R(T)$ curve at $\mu_0 H = 6$ mT in the inset of Fig. 1 (d).

Fig. 2 (e) shows temperature dependencies of critical currents. The I_c vanishes sharply with a negative curvature $d^2 I_c / dT^2 < 0$ at $T \rightarrow T_c(\text{Nb})$. This is the third indication that there is no deteriorated surface layer at the BNFA crystal interface. Indeed, a deteriorated non-superconducting (normal metal) layer would lead to appearance of the proximity effect, which usually leads to a positive curvature of $I_c(T)$ at $T \rightarrow T_c$ [46, 48–50]. The observed negative curvature along with the sharp resistive transition of the BNFA interface beneath the junction at the bulk $T_c(\text{BNFA})$, see Fig. 1 (d), and the absence of the excess current in the I - V characteristics, see Fig. 1 (f), prove the absence of surface deterioration and proximity effect in our junctions and confirm that we probe bulk order parameter in the BNFA crystal.

As follows from the scaling of I_c vs. area in Fig. 1 (f), all junctions have the same critical current density $J_c \simeq 3 \times 10^3$ A/cm². It is large enough to question the d -wave symmetry of the order parameter in BNFA (see extra discussion in the Supplementary [41]). The s_{++} case would naturally lead to a large J_c . But for the s_{\pm} scenario at least a partial compensation of supercurrents from the sign-reversal bands, leading to suppression of J_c [28, 34]. The critical current is not universal. The proper quantity for analysis is the $I_c R_n$ product. For junctions between s -wave superconductors, including the s_{++} case, the $I_c R_n$ is determined by the nearly universal (transparency independent) Ambegaokar-Baratoff expression $e I_c R_n(T=0) = a \Delta$, [39], where a is a constant of order unity. In our case the smallest gap is $\Delta_{Nb} \simeq 1.5$ meV. Thus in the s_{++} case we would anticipate the $I_c R_n$ of the order of mV, while for the s_{\pm} it should be smaller.

The inset in Fig. 2 (f) shows $I_c R_n$ products at $T = 3.6$ K. It is seen that $I_c R_n \simeq 3 \mu\text{V}$ is similar for all junctions. A systematic decrease in the smallest junctions can be explained by the influence of noise and thermal fluctuations [44, 51], which suppress the switching current due to a proportional-to-area reduction of the Josephson energy. Therefore, we conclude that there is a good consistency of the data. A remarkable fact is that the $e I_c R_n$ is extremely small, ~ 500 times smaller than the gap in Nb. Such a small value, with no sign of the proximity effect in our junctions, essentially precludes the s_{++} symmetry in the studied pnictide.

To understand if our results are consistent with the s_{\pm} symmetry, we refer to theoretical analysis made by Burmistrova et al. [28]. In case of coherent tunneling, tunneling probability depends on the band structures and shapes of the corresponding Fermi surfaces. In pnictides

one of the bands is placed in the center while the other at the edge of the Brillouin zone, see Fig. 1 (a). Supercurrents from the two sign-reversal s_{\pm} bands oppose each other, reducing the total critical current. But the extent to which they compensate each other depends on several factors: (i) Hopping probabilities from the two bands; (ii) Momentum selectivity: the tunnel current depends on the value of the in-plane momentum k_{\parallel} . Since the two bands in the pnictide do not overlap, for each k_{\parallel} only one of the bands contributes to the electronic transport and which one and how much depends on the size/shape of the receiving s -wave Fermi surface. (iii) The momentum selectivity depends on the transparency of the barrier: increasing the thickness of the barrier leads to predominance of tunneling of electrons with large k_{\perp} and thus reduces the contribution from the band with large k_{\parallel} at the edges of the Brillouin zone.

The main panel in Fig. 2 (f) shows normalized temperature dependence of $I_c R_n$ for several junctions. It provides another clue about the gap symmetry in BNFA. The dotted line in Fig. 2 (f) represents the Ambegaokar-Baratoff [39] $I_c R_n(T)$ dependence, expected for s/s' junctions (data from Ref. [28]). It is clearly different from the reported experimental $I_c R_n(T)$ dependence, which exhibits a more rapid fall-off at low $T \gtrsim 2$ K. The dashed line in Fig. 2 (f) represents the theoretical $I_c R_n(T)$ dependence for a s/s_{\pm} junction from Fig. 11 (c) of Ref. [28]. Apparently, it fits quantitatively to the measured $I_c R_n(T)$ dependence, including all the characteristic deviations from the Ambegaokar-Baratoff dependence. Furthermore, the theoretical curve corresponds to the case of almost complete compensation of opposite supercurrents from the two sign-reversal bands. This is fully consistent with the observed very small absolute value of $e I_c R_n(0) \simeq 3 \mu\text{eV}$, 500 times smaller than the smallest $\Delta_{Nb} \simeq 1.5$ meV. This implies that there is indeed an almost complete (to a sub-percent level) cancellation of the Josephson current in our Nb/BNFA junctions.

To conclude, we fabricated and studied high-quality Josephson junctions between c -axis oriented $\text{Ba}_{1-x}\text{Na}_x\text{Fe}_2\text{As}_2$ and an s -wave Nb. Junctions show a Josephson current density $\sim 10^3$ A/cm², which is large enough to preclude the pure d -wave symmetry of the order parameter in the pnictide. However, the $I_c R_n$ product is very small $\simeq 3 \mu\text{V}$, not consistent with the s_{++} symmetry either. We emphasize that the inconsistency is not marginal but is almost three orders of magnitude. So large discrepancy with no signs of the proximity effect and along with the observed unusual temperature dependence provide strong evidence for the s_{\pm} symmetry of the order parameter in $\text{Ba}_{1-x}\text{Na}_x\text{Fe}_2\text{As}_2$. It is the phase sensitivity of our c -axis oriented Nb/BNFA junctions that leads to an almost complete (down to a sub-percent) cancellation of opposite supercurrents from the sign-reversal s_{\pm} bands in the pnictide.

The work was supported by the Swedish Foundation for International Cooperation in Research and Higher Education (STINT) Grant No. IG2013-5453, the Swedish Research Council (VR) Grant No. 621-2014-4314, the project No. 6250 by the Science and Technology Center in Ukraine (STCU) and the National Academy of Science of Ukraine (NASU). We are grateful to S. Aswartham, S. Wurmehl and B. Büchner for providing BNFA single crystals, to T. Golod, A. Iovan and the Core Facility in Nanotechnology at Stockholm University for technical support with sample fabrication.

* Vladimir.Krasnov@fysik.su.se

- [1] C. C. Tsuei and J. R. Kirtley, Pairing symmetry in cuprate superconductors, *Rev. Mod. Phys.* **72**, 969 (2000).
- [2] A. Chubukov, *An. Rev. Cond. Matt. Phys.* **3**, 57 (2012).
- [3] P. J. Hirschfeld, M. M. Korshunov, and I. I. Mazin, Gap symmetry and structure of Fe-based superconductors, *Rep. Prog. Phys.* **74**, 124508 (2011).
- [4] D. A. Wollman, D. J. Van Harlingen, W. C. Lee, D. M. Ginsberg, and A. J. Leggett, Experimental determination of the superconducting pairing state in YBCO from the phase coherence of YBCO-Pb dc SQUIDS, *Phys. Rev. Lett.* **71**, 2134 (1993).
- [5] T. K. Ng and N. Nagaosa. Broken time-reversal symmetry in Josephson junction involving two-band superconductors, *EPL* **87**, 17003 (2009).
- [6] J. Linder, I. B. Sperstad, and A. Sudbø. $0-\pi$ phase shifts in Josephson junctions as a signature for the s_{\pm} -wave pairing state, *Phys. Rev. B* **80**, 020503(R) (2009).
- [7] Y. Ota, M. Machida, T. Koyama, and H. Matsumoto. Theory of Heterotic Superconductor-Insulator-Superconductor Josephson Junctions between Single- and Multiple-Gap Superconductors, *Phys. Rev. Lett.* **102**, 237003 (2009).
- [8] S. Kasahara, H. J. Shi, K. Hashimoto, S. Tonegawa, Y. Mizukami, T. Shibauchi, K. Sugimoto, T. Fukuda, T. Terashima, A. H. Nevidomskyy, and Y. Matsuda, Electronic nematicity above the structural and superconducting transition in $\text{BaFe}_2(\text{As}_{1-x}\text{P}_x)_2$, *Nature* **486**, 382 (2012).
- [9] J.-H. Chu, J. G. Analytis, K. De Greve, P. L. McMahon, Z. Islam, Y. Yamamoto, and I. R. Fisher, In-Plane Resistivity Anisotropy in an Underdoped Iron Arsenide Superconductor, *Science* **329**, 824 (2010).
- [10] M. A. Tanatar, E. C. Blomberg, A. Kreyssig, M. G. Kim, N. Ni, A. Thaler, S. L. Budko, P. C. Canfield, A. I. Goldman, I. I. Mazin, and R. Prozorov, Uniaxial-strain mechanical detwinning of CaFe_2As_2 and BaFe_2As_2 crystals: Optical and transport study, *Phys. Rev. B* **81**, 184508 (2010).
- [11] M. D. Watson, T. K. Kim, A. A. Haghighirad, N. R. Davies, A. McCollam, A. Narayanan, S. F. Blake, Y. L. Chen, S. Ghannadzadeh, A. J. Schofield, M. Hoesch, C. Meingast, T. Wolf, and A. I. Coldea, Emergence of the nematic electronic state in FeSe, *Phys. Rev. B* **91**, 155106 (2015).
- [12] K. Nakayama, Y. Miyata, G. N. Phan, T. Sato, Y. Tanabe, T. Urata, K. Tanigaki, and T. Takahashi, Reconstruction of Band Structure Induced by Electronic Nematicity in an FeSe Superconductor, *Phys. Rev. Lett.* **113**, 237001 (2014).
- [13] S.-H. Baek, D. V. Efremov, J. M. Ok, J. S. Kim, J. van den Brink, and B. Büchner, Orbital-driven nematicity in FeSe, *Nat. Mater.* **14**, 210 (2015).
- [14] T. M. McQueen, A. J. Williams, P. W. Stephens, J. Tao, Y. Zhu, V. Ksenofontov, F. Casper, C. Felser, and R. J. Cava, Tetragonal-to-Orthorhombic Structural Phase Transition at 90 K in the Superconductor $\text{Fe}_{1.01}\text{Se}$, *Phys. Rev. Lett.* **103**, 057002 (2009).
- [15] W. Lv, J. Wu, and P. Phillips, Orbital ordering induces structural phase transition and the resistivity anomaly in iron pnictides, *Phys. Rev. B* **80**, 224506 (2009).
- [16] R. M. Fernandes, A. V. Chubukov, and J. Schmalian, What drives nematic order in iron-based superconductors?, *Nat. Phys.* **10**, 97 (2014).
- [17] H. Kontani and S. Onari, Orbital-Fluctuation-Mediated Superconductivity in Iron Pnictides: Analysis of the Five-Orbital Hubbard-Holstein Model, *Phys. Rev. Lett.* **104**, 157001 (2010).
- [18] A. D. Christianson, E. A. Goremychkin, R. Osborn, S. Rosenkranz, M. D. Lumsden, C. D. Malliakas, I. S. Todorov, H. Claus, D. Y. Chung, M. G. Kanatzidis, R. I. Bewley, and T. Guidi, Unconventional superconductivity in $\text{Ba}_{0.6}\text{K}_{0.4}\text{Fe}_2\text{As}_2$ from inelastic neutron scattering, *Nature* **456**, 930 (2008).
- [19] M. D. Lumsden, A. D. Christianson, D. Parshall, M. B. Stone, S. E. Nagler, G. J. MacDougall, H. A. Mook, K. Lokshin, T. Egami, D. L. Abernathy, E. A. Goremychkin, R. Osborn, M. A. McGuire, A. S. Sefat, R. Jin, B. C. Sales, and D. Mandrus, Two-dimensional resonant magnetic excitation in $\text{BaFe}_{1.84}\text{Co}_{0.16}\text{As}_2$, *Phys. Rev. Lett.* **102**, 107005 (2009).
- [20] D. S. Inosov, J. T. Park, P. Bourges, D. L. Sun, Y. Sidis, A. Schneidewind, K. Hradil, D. Haug, C. T. Lin, B. Keimer, and V. Hinkov, Normal-state spin dynamics and temperature-dependent spin-resonance energy in optimally doped $\text{BaFe}_{1.85}\text{Co}_{0.15}\text{As}_2$, *Nat. Phys.* **6**, 178 (2010).
- [21] D. S. Inosov, S. V. Borisenko, I. Eremin, A. A. Kordyuk, V. B. Zabolotnyy, J. Geck, A. Koitzsch, J. Fink, M. Knupfer, B. Büchner, H. Berger, and R. Follath, Relation between the one-particle spectral function and dynamic spin susceptibility of superconducting $\text{Bi}_2\text{Sr}_2\text{CaCu}_2\text{O}_{8-d}$, *Phys. Rev. B* **75**, 172505 (2007).
- [22] S. Onari, H. Kontani, and M. Sato, Structure of neutron-scattering peaks in both s_{++} -wave and s_{\pm} -wave states of an iron pnictide superconductor, *Phys. Rev. B* **81**, 060504 (2010).
- [23] Y. Zhang, Z. R. Ye, Q. Q. Ge, F. Chen, J. Jiang, M. Xu, B. P. Xie, and D. L. Feng, Nodal superconducting-gap structure in ferropnictide superconductor $\text{BaFe}_2(\text{As}_{0.7}\text{P}_{0.3})_2$, *Nat. Phys.* **8**, 371 (2012).
- [24] J. K. Dong, S. Y. Zhou, T. Y. Guan, H. Zhang, Y. F. Dai, X. Qiu, X. F. Wang, Y. He, X. H. Chen, and S. Y. Li, Quantum Criticality and Nodal Superconductivity in the FeAs-Based Superconductor KFe_2As_2 , *Phys. Rev. Lett.* **104**, 087005 (2010).
- [25] D. V. Evtushinsky, V. B. Zabolotnyy, T. K. Kim, A. A. Kordyuk, A. N. Yaresko, J. Maletz, S. Aswartham, S. Wurmehl, A. V. Boris, D. L. Sun, C. T. Lin, B. Shen, H. H. Wen, A. Varykhalov, R. Follath, B. Büchner, and S. V.

- Borisenko, Strong electron pairing at the iron $3d_{xz,yz}$ orbitals in hole-doped BaFe_2As_2 superconductors revealed by angle-resolved photoemission spectroscopy, *Phys. Rev. B* **89**, 064514 (2014).
- [26] C.-T. Chen, C. C. Tsuei, M. B. Ketchen, Z.-A. Ren, and Z. X. Zhao, Integer and half-integer flux-quantum transitions in a niobium-iron pnictide loop, *Nat. Phys.* **6**, 260 (2010).
- [27] S. Schmidt, S. Döring, N. Hasan, F. Schmidl, V. Tympe, F. Kurth, K. Iida, H. Ikuta, T. Wolf, and P. Seidel, Josephson effects at iron pnictide superconductors: Approaching phase-sensitive experiments, *Phys. Stat. Sol. B* **254**, 1600165 (2017).
- [28] A. V. Burmistrova, I. A. Devyatov, A. A. Golubov, K. Yada, Y. Tanaka, M. Tortello, R. S. Gonnelli, V. A. Stepanov, X. Ding, H. H. Wen, and L. H. Green. Josephson current in Fe-based superconducting junctions: Theory and experiment, *Phys. Rev. B* **91**, 214501 (2015). We note that the $I_c(T)$ in s/s_{\pm} junctions does depend on the crystallographic orientation of the pnictide and interface transparency. Therefore, detailed quantitative “fit” to the data is not an unambiguous evidence as such. But the qualitative deviation from the Ambegaokar-Baratoff dependence is indicative.
- [29] V. V. Fisun, O. P. Balkashin, O. E. Kvitnitskaya, I. A. Korovkin, N. V. Gamayunova, S. Aswartham, S. Wurmehl, and Yu. G. Naidyuk. Josephson effect and Andreev reflection in $\text{Ba}_{1-x}\text{Na}_x\text{Fe}_2\text{As}_2$ ($x=0.25$ and 0.35) point contacts. *Low Temp. Phys.* **40**, 919 (2014).
- [30] T. Golod, A. Rydh, and V. M. Krasnov, Detection of the Phase Shift from a Single Abrikosov Vortex, *Phys. Rev. Lett.* **104**, 227003 (2010).
- [31] Y. Mizukami, M. Konczykowski, Y. Kawamoto, S. Kurata, S. Kasahara, K. Hashimoto, V. Mishra, A. Kreisel, Y. Wang, P.J. Hirschfeld, Y. Matsuda, and T. Shibauchi, Disorder-induced topological change of the superconducting gap structure in iron pnictides, *Nat. Commun.* **5**, 5657 (2014).
- [32] S. Chi, S. Johnston, G. Levy, S. Grothe, R. Szedlak, B. Ludbrook, R. Liang, P. Dosanjh, S. A. Burke, A. Damascelli, D. A. Bonn, W. N. Hardy, and Y. Pennec, Sign inversion in the superconducting order parameter of LiFeAs inferred from Bogoliubov quasiparticle interference, *Phys. Rev. B* **89**, 104522 (2014).
- [33] P. J. Hirschfeld, D. Altenfeld, I. Eremin, and I. I. Mazin, Robust determination of the superconducting gap sign structure via quasiparticle interference, *Phys. Rev. B* **92**, 184513 (2015).
- [34] A. E. Koshelev, Phase diagram of Josephson junction between s and s_{\pm} superconductors in the dirty limit. *Phys. Rev. B* **86**, 214502 (2012).
- [35] S. Aswartham, M. Abdel-Hafiez, D. Bombor, M. Kumar, A. U. B. Wolter, C. Hess, D. V. Evtushinsky, V. B. Zabolotnyy, A. A. Kordyuk, T. K. Kim, S. V. Borisenko, G. Behr, B. Büchner, and S. Wurmehl, Hole doping in BaFe_2As_2 : The case of $\text{Ba}_{1-x}\text{Na}_x\text{Fe}_2\text{As}_2$ single crystals, *Phys. Rev. B* **85**, 224520 (2012).
- [36] S. Avci, J.M. Allred, O. Chmaissem, D.Y. Chung, S. Rosenkranz, J.A. Schlueter, H. Claus, A. Daoud-Aladine, D.D. Khalyavin, P. Manuel, A. Llobet, M.R. Suchomel, M.G. Kanatzidis, R. Osborn, Structural, magnetic, and superconducting properties of $\text{Ba}_{1-x}\text{Na}_x\text{Fe}_2\text{As}_2$, *Phys. Rev. B* **88**, 094510 (2013).
- [37] V. B. Zabolotnyy, D. S. Inosov, D. V. Evtushinsky, A. Koitzsch, A. A. Kordyuk, G. L. Sun, J. T. Park, D. Haug, V. Hinkov, A. V. Boris, C. T. Lin, M. Knupfer, A. N. Yaresko, B. Büchner, A. Varykhalov, R. Follath, and S. V. Borisenko, (π, π) electronic order in iron arsenide superconductors, *Nature* **457**, 569 (2009).
- [38] D. V. Evtushinsky, D. S. Inosov, V. B. Zabolotnyy, M. S. Viazovska, R. Khasanov, A. Amato, H.-H. Klauss, H. Luetkens, Ch. Niedermayer, and G. L. Sun, Momentum-resolved superconducting gap in the bulk of $\text{Ba}_{1-x}\text{K}_x\text{Fe}_2\text{As}_2$ from combined ARPES and SR measurements, *New J. Phys.* **11**, 055069 (2009).
- [39] V. Ambegaokar and A. Baratoff, Tunneling in superconductors, *Phys. Rev. Lett.* **10**, 486 (1963).
- [40] Y. Tanaka and S. Kashiwaya, Theory of Josephson effects in anisotropic superconductors, *Phys. Rev. B* **56**, 892 (1997). We note that a second-harmonic current between s and d wave superconductors is possible, but this is inconsistent with our data, as discussed in the Supplementary [41].
- [41] See EPAPS Document No.XXX. The supplementary contains additional information about sample fabrication, characterization, a summary of junction characteristics and a discussion of the junction interface, which includes Refs. [42–44]
- [42] Y. Liu, M. A. Tanatar, W. E. Straszheim, B. Jensen, K. W. Dennis, R. W. McCallum, V. G. Kogan, R. Prozorov, and T. A. Lograsso, Comprehensive scenario for single-crystal growth and doping dependence of resistivity and anisotropic upper critical fields in $(\text{Ba}_{1-x}\text{K}_x)\text{Fe}_2\text{As}_2$ ($0.22 \leq x \leq 1$), *Phys. Rev. B* **89**, 134504 (2014).
- [43] S.Y. Xu, et al., Discovery of Weyl fermion state with Fermi arcs in niobium arsenide. *Nature Physics* **11**, 748 (2015).
- [44] V. M. Krasnov, T. Golod, T. Bauch, and P. Delsing, Anticorrelation between temperature and fluctuations of the switching current in moderately damped Josephson junctions. *Phys. Rev. B* **76**, 224517 (2007).
- [45] A. A. Kalenyuk, A. Pagliaro, E. A. Borodianskyi, S. Aswartham, S. Wurmehl, B. Büchner, D. A. Chareev, A. A. Kordyuk, and V. M. Krasnov, Unusual two-dimensional behavior of iron-based superconductors with low anisotropy, *Phys. Rev. B* **96**, 134512 (2017).
- [46] A. A. Golubov, V.M. Krasnov, and M. Yu. Kupriyanov, The constriction model for SNS Josephson junctions, *J. Low Temp. Phys.* **106**, 249 (1997).
- [47] V.M. Krasnov, V. A. Oboznov, and N.F. Pedersen, Fluxon dynamics in long Josephson junctions in the presence of a temperature gradient or spatial nonuniformity, *Phys. Rev. B* **55**, 14486 (1997).
- [48] A.A. Golubov, E.P. Houwman, J.G. Gijsbertsen, V.M. Krasnov, J. Flokstra, H. Rogalla, and M. Yu. Kupriyanov, Proximity effect in superconductor-insulator-superconductor tunnel junction: Theory and experiment, *Phys. Rev. B* **51**, 1073 (1995).
- [49] L. Yu, R. Gandikota, R. K. Singh, L. Gu, D. J. Smith, X. Meng, X. Zeng, T. Van Duzer, J. M. Rowell and N. Newman, Internally shunted Josephson junctions with barriers tuned near the metalinsulator transition for RSFQ logic applications, *Supercond. Sc. Technol.* **19**, 719 (2006).
- [50] B. Baek, P. D. Dresselhaus, and S. P. Benz, Co-Sputtered Amorphous $\text{Nb}_x\text{Si}_{1-x}$ Barriers for Josephson-Junction Circuits, *IEEE Trans. Appl. Supercond.* **16**, 1966 (2006).
- [51] J. M. Martinis, M. H. Devoret, and J. Clarke. Experi-

mental tests for the quantum behavior of a macroscopic

degree of freedom: The phase difference across a Josephson junction, *Phys. Rev. B* **35**, 4682 (1987).